Geological Quarterly, 2021, 65: 30
DOI: http://dx.doi.org/10.7306/gq.1598

A strongly positive sulphur isotopic shift in late Ediacaran-early Cambrian seawater: evidence from evaporites in the Salt Range Formation, northern Pakistan

Fanwei MENG[1], Zhili ZHANG[2], Krzysztof BUKOWSKI[3, *], Qingong ZHUO[4], Naveed AHSAN[5], Saif UR-REHMAN[5] and Pei Ni[6]

[1] Chinese Academy of Sciences, Nanjing Institute of Geology and Palaeontology, State Key Laboratory of Palaeobiology and Stratigraphy, Nanjing, 210008, China

[2] Petroleum Exploration and Development Research Institute, SINOPEC, 100083, Beijing, China

[3] AGH University of Science and Technology, Faculty of Geology, Geophysics and Environmental Protection, Al. A. Mickiewicza 30, 30-059 Kraków, Poland

[4] Research Institute of Petroleum Exploration and Development, CNPC, Beijing, 100083, China

[5] University of the Punjab, Institute of Geology, Quaid-e-Azam Campus, Lahore 54590, Pakistan

[6] Nanjing University, School of Earth Sciences and Engineering, Institute of Geo-Fluids, State Key Laboratory for Mineral Deposit Research, Nanjing, 210093, China

Meng, F., Zhang, Z., Bukowski, K., Zhuo, Q., Ahsan, N., Ur-Rehman S., Ni, P., 2021. A strongly positive sulphur isotopic shift in late Ediacaran-early Cambrian seawater: evidence from evaporites in the Salt Range Formation, northern Pakistan. Geological Quarterly, 2021, 65: 30, doi: 10.7306/gq.1598

The Salt Range Formation in northern Pakistan is globally well-known for its extremely large evaporite deposits dated to the upper Ediacaran–lower Cambrian. This huge evaporite belt formed an area covering present-day parts of India, Pakistan, Iran, Oman, and even South China (~200,000 km^2 in South China). Sulphate minerals, including anhydrite and gypsum, can continuously record seawater sulphur isotopic composition. Until now, there was only one dataset reporting the isotopic composition of evaporites in Pakistan. This study reports new data, which points to a strongly positive sulphur isotopic shift (>+30‰, VCDT values) in the Salt Range Formation in Pakistan. Based on the stratigraphic position, similarity in lithology, age, and sulphur isotope data of the evaporitic sequences, it can be inferred that the Neoproterozoic Indo-Pakistan Plate and the Yangtze Platform were closely related palaeogeographically during the terminal Neoproterozoic. This interpretation can improve understanding of the palaeogeographical evolution of the area during the Neoproterozoic, with particular reference to the origin of biogeochemical cycles and the diagenetic evolution of the evaporitic deposits.

Key words: sulphur isotope, gypsum, Salt Range Formation, Indo-Pakistan Plate, South China, Yangtze Block.

INTRODUCTION

The terminal Neoproterozoic (Ediacaran) to early Cambrian was a period in Earth's history when huge evaporite deposits accumulated in India, Pakistan, Iran, Oman, and South China in rift basins (Knauth, 1998, 2005; Meng et al., 2011a, b; Cui et al., 2015, 2016; Warren, 2016). Evaporites retain a wealth of information about the prevailing temperature, climate, and chemistry of ancient seas and saline lakes (e.g., Benison, 1995; Kovalevich et al., 1998; Shields et al., 1999; Bukowski et al., 2000, 2007; Losey and Benison, 2000; Lowenstein et al., 2001; Kovalevych et al., 2002, 2006, 2009; Galamay et al., 2003, 2020; Petrychenko and Peryt, 2004; Petrychenko et al., 2005; Satterfield et al., 2005; Meng et al., 2011a, b, 2012, 2014, 2018; Spear et al., 2014). In particular, the processes of precipitation, diagenesis, and weathering do not cause notable fractionation of the sulphur isotopes in ancient evaporite deposits (Hoefs, 2004; Jaworska and Wilkosz, 2012). This fact has been well-substantiated through laboratory experiments (e.g., Thode et al., 1961; Raab and Spiro, 1991) in which it has been found that sulphur isotope fractionation during the precipitation of evaporites is negligible (0–2.6‰). Moreover, the sulphur isotopic ratio ($\delta^{34}S/\delta^{32}S$) for present-day marine evaporites conforms to that of seawater (Claypool et al., 1980).

Therefore, marine sulphur as sulphate (SO_4^{-2}) associated with evaporite deposits (sedimentary gypsum or anhydrite) can be used to reliably determine temporal variations in the $\delta^{34}S$ composition of ancient seawater, including during the terminal Neoproterozoic (Holser and Kaplan, 1966; Claypool et al., 1980; Holser, 1984; Holser et al., 1988; Strauss et al., 2001; Strauss, 2003; Kampschulte and Strauss, 2004; Mazumdar and Strauss, 2006; Present et al., 2020).

* Corresponding author, e-mail: buk@agh.edu.pl

Received: January 2, 2021; accepted: May 1, 2021; first published online: June 16, 2021

Evaporites can form in multiple geological settings from marine and non-marine brines (Warren, 2016; Li et al., 2018). The oldest recrystallized halites have been reported from the Bitter Springs Formation (840–830 Ma) in Australia (Kovalevych et al., 2006), and the oldest anhydrite from the Paleoproterozoic (~2.1 Ga) Dashiqiao Formation in China (Chen et al., 2003; Dong et al., 2016). The various evaporite and carbonate deposits along Gondwanan supercontinental margins were formed near the equator during the late Neoproterozoic Ediacaran to early Cambrian time. They have been recorded in Iran and the Persian Gulf (Hormuz Salt Formation), from the region of Oman and Qatar (Ara Salt Formation), as well as Pakistan (Salt Range Formation). These evaporite-bearing formations constitute part of the evaporite belt reconstructed by Husseini and Husseini (1990), in which Oman is located to the west of the belt and India is at its eastern edge. A Late Neoproterozoic to early Cambrian age has generally been assigned to the Hanseran Evaporite Group (India) based on halite and lithological similarities to the Salt Range Formation of Pakistan (Jones, 1970; Strauss et al., 2001).

The Salt Range and Hanseran formations represent the easternmost evaporite deposits in northwestern Pakistan and India (Jones, 1970; Husseini and Husseini, 1990; Grelaud et al., 2002; Jiang et al., 2003; Hussain et al., 2020, 2021). The Salt Range Formation in Pakistan is well-exposed, and its presence has been reported from various boreholes drilled on the Potwar Plateau and Punjab Platform (Fig. 1). This formation is composed of gypsiferous marls, halite, dolomite and oil shales, and unconformably overlies presumed Precambrian metamorphic rocks. Its upper contact is with the Cambrian sequence that terminates unconformably at the Permian and is marked by glacial tillites (Ahmad and Alam, 2007; Khan et al., 2020).

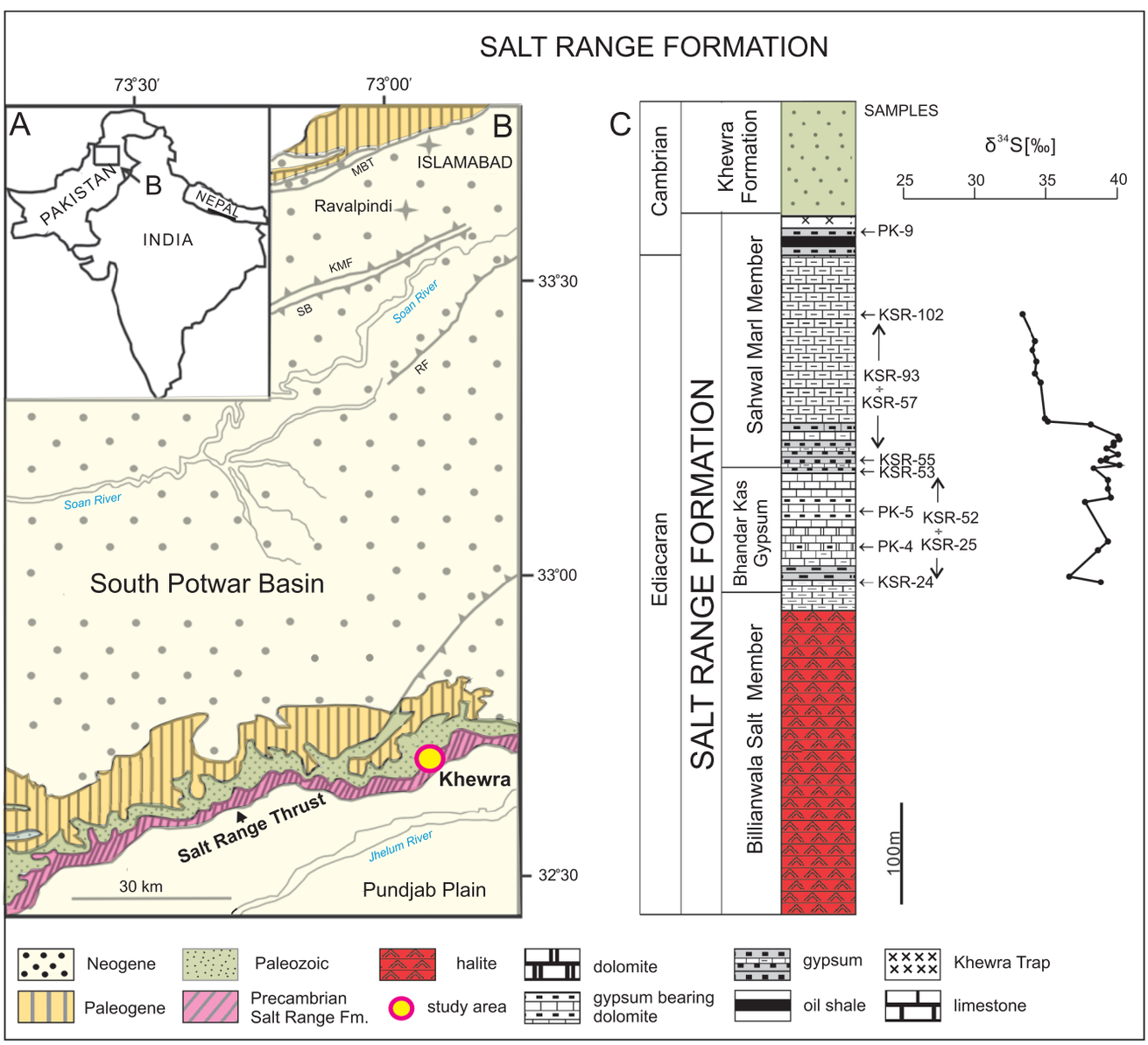

Fig. 1. Map of the South Potwar Basin (A, B) showing the location and sulphur stable isotopes of the gypsum samples from the Salt Range Formation (C)

KMF – Khari Murat Fault, MBT – Main Boundary Thrust, RF – Riwat Fault, SB – Soan Back Thrust (after Grelaud et al., 2002)

The sulphur ($\delta^{34}S$) isotope composition of the evaporite deposits in the Hanseran Formation (India) shifts strongly to +30‰ (Strauss et al., 2001). However, a review of the relevant literature (Gee, 1945; Asrarullah, 1967; Fatmi, 1973; Shah, 1977, 2009) indicates that no substantial research has been conducted on the sulphur isotope composition of the Salt Range Formation. If the sulphur isotope positive anomaly is recorded in the evaporite succession in Pakistan, this could be considered an important correlation event – if it indeed represents a global geochemical anomaly. In this study, we determine the sulphur ($\delta^{34}S$) isotope composition of the evaporite deposits dating from the late Ediacaran–early Cambrian in Pakistan and compare them with data from Proterozoic-lower Cambrian formations from South China and NW India in order to address this question.

GEOLOGICAL SETTING

Evaporites of the "saline series" of Wynne (1878) and "Punjab saline series" of Gee (1945) have been referred to the Salt Range Formation (Asrarullah, 1967; Fatmi, 1973). Asrarullah (1967) divided the Salt Range Formation into three members; in chronostratigraphic order (from base to top), are (1) the Billianwala Salt, (2) Bhandar Kas Gypsum, and (3) the Sahwal Marl (Fig. 1). The Billianwala Salt Member comprises red, ferruginous marl with thick seams of salt and a total thickness of ~650 m at the type locality. The Bhandar Kas Gypsum Member is composed of ~80 m thick massive gypsum, with minor dolomite beds embedded in shales. The 140 m thick Sahwal Marl Member consists of dull and bright red marls with seams of gypsum and salt. Near the apex of Sahwal Marl Member, the marls were intruded by the Khewra Trap/Khewrite volcanic flow. Moreover, ~20 cm of oil shales appear on top of the Sahwal marl. At its type locality, the Sahwal Marl Member is ~140 m thick.

The Salt Range Formation is well-exposed from east (Kussak, Pakistan) to west (Kalabagh) along the southern margin of the Salt Range (Fig. 1). This formation is also encountered in various boreholes drilled on the Potwar Plateau and Punjab Platform (Kadri, 1995; Ahsan et al., 2013). The base of the Salt Range Formation is only well-known from Karampur, where it overlies metamorphic rocks, possibly those of the Precambrian Kirana complex. The evaporites lack fossils throughout the formation; thus, their age can only be constrained using radiometric methods (Chaudhuri and Clauer, 1992; Shah, 2009). However, the Salt Range Formation age is still debated, although it is conformably overlain by the lower Cambrian Khewra Sandstone (Shah, 2009). The abnormally high seawater sulphur isotopic data (+30 to +35‰, and sometimes up to 45‰) from the upper Neoproterozoic–Cambrian marine evaporites could be used to constrain the age of the formation (Strauss et al., 2001; Paytan et al., 2012).

Husseini and Husseini (1990) suggested that the Salt Range Formation, which is similar to the Hormuz Salt Formation, was created in evaporite basins along Gondwanan supercontinental margins in late Neoproterozoic to early Cambrian times (Allen, 2007; Fig. 2). Volcanic rocks accompanying the evaporites were formed in the Late Ediacaran, as shown by radiometric dating of zircons from an exposure of rhyolites on the island of Hormuz, indicating an age of 558 ±7 Ma (Faramarzi et al., 2015) and zircon ages of igneous rocks from the Hormuz Formation in the Jahani salt diapir gave an age of 547 ±6 Ma (Alavi, 2004).

MATERIALS AND METHODS

Samples of pure gypsum were collected from two sections through an outcrop of the Bhandar Kas Gypsum Member in the Salt Range Formation from its type locality at Khewra Gorge (Fig. 1; Tables 1 and 2). Eight samples were collected from the first section of the Bhandar Kas Gypsum; one sample (9) came from the gypsum at the top of the oil shales (Table 1). In addition, 27 samples were collected from the second section, including 12 samples from the Bhandar Kas Gypsum (KSR-24 to KSR-53) and 15 samples (KSR-55 to KSR-102) from the Sahwal Marl (Table 2 and Fig. 3).

Samples from the first section were processed with the methods outlined by Strauss et al. (2001), who obtained pure anhydrite or sulphate-halite mixtures from several boreholes. The former is analysed directly, and the latter is analysed by adding barium chloride to precipitate barium sulphate after dissolution. The methods employed to analyse sulphur isotopes

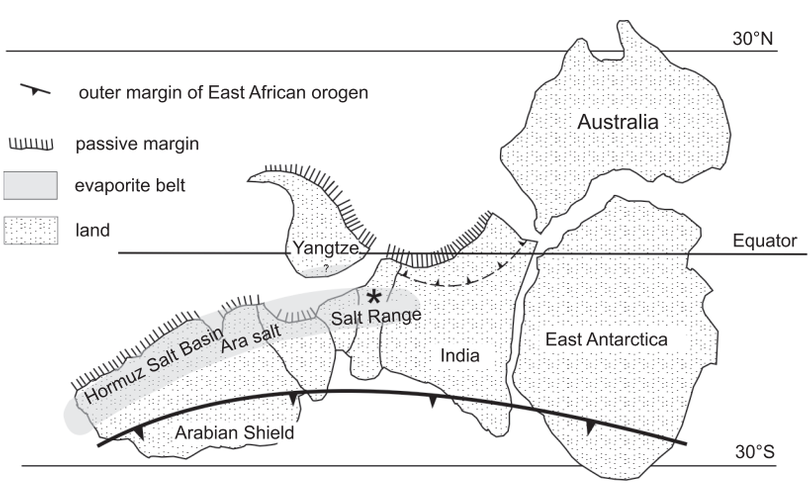

Fig. 2. Positions of the Salt Range Formation in the evaporitic belt, the Indian Shield, and the Yangtze Block (South China) during the Neoproterozoic (after Jiang et al., 2003; Allen, 2007; Craig et al., 2009)

Table 1

Gypsum samples collected from the first section through the Salt Range Formation (Bhandar Kas Gypsum/Sahwal Marl) and their sulphur isotope data

Samples (from top to base)	Lithology	$\delta^{34}S$ [‰]	Member
Sample-9	pure white gypsum	37.6	Sahwal Marl
Sample-5	pure white gypsum	34.3	Bhandar Kas Gypsum
Sample-4*	thick gypsum		Bhandar Kas Gypsum
Pk-4-6	pure white gypsum	32.8	Bhandar Kas Gypsum
Pk-4-5	pure white gypsum	34.1	Bhandar Kas Gypsum
Pk-4-4	pure white gypsum	32.1	Bhandar Kas Gypsum
Pk-4-3	pure white gypsum	32.8	Bhandar Kas Gypsum
Pk-4-2	pure white gypsum	32.9	Bhandar Kas Gypsum
Pk-4-1	pure white gypsum	32.4	Bhandar Kas Gypsum
S.L.- 120-T63-40	pure white gypsum	38.2	Salt Range Fm. (after Sakai, 1972)

Samples Pk-4-1, Pk-4-2, Pk-4-3, Pk-4-4, Pk-4-5, Pk-4-6 come from one level in the thick gypsum section, sample-9 comes from within the oil shales, the boundary of upper Neoproterozoic-lower Cambrian; data for sample S.L.-120-T63-40 comes from Sakai (1972); * – due to the large thickness was divided into Pk-4-1, Pk-4-2, Pk-4-3, Pk-4-4, Pk-4-5; Pk-4-6

were modified after Hałas and Szaran (1999). Approximately 15 mg of $CaSO_4$ was mixed with $NaPO_3$ (150 mg) and combusted in the presence of copper turnings (150 mg). A vacuum was created for conversion to sulphur dioxide at 750°C for 15 minutes. These analyses were conducted at the Institute of Geology and Geophysics, Chinese Academy of Sciences (IGG-CAS) on a *Finnigan Delta-S* gas-source mass spectrometer. $\delta^{34}S$ data were calibrated relative to the *Vienna-Canyon Diablo Troilite* scale using IAEA standards NBS 127 (+20.3‰) IAEA-SO-5 (+0.5‰) and IAEA-SO-6 (–34.1‰), and the sulphur isotope results were generally reproducible within ±0.3‰.

Twenty-seven pure gypsum samples collected from the second section (Table 2) were processed following the methods outlined by Meng et al. (2019). Analysis for determining stable isotopes of sulphur was carried out at the Oxy-Anion Stable Isotope Consortium (OASIC) at Louisiana State University, USA. Gypsum samples were powdered and dissolved in 30 mL 1N HCl with continuous shaking. The slurry was decanted and vacuum filtered through a 0.45 μm cellulose membrane filter. Supernatants were transferred to 50 ml centrifuge tubes and precipitated as $BaSO_4$ by adding 3 mL saturated $BaCl_2$ solution. Sulphur isotope analyses were conducted via an *Isoprime100* (*Isoprime 100*, UK) gas source mass spectrometer fitted with a peripheral elemental analyzer (*Micro Vario Cube* UK). About 0.2–0.3 mg of powdered samples were placed into tin capsules, mixed with excess V_2O_5, and combusted at 1050°C to produce SO_2, which was then measured by the spectrometer. All isotope measurements are expressed in delta notation relative to *Vienna Canyon Diablo Troilite* (V-CDT) isotopic standard.

Analytical errors were <0.3‰, calculated from replicate analyses of samples and laboratory standards. Isotopic standards were used to construct calibration curves for linear and two-point corrections. The values were calibrated using standards of barium sulphate ($LSU\text{-}BaSO_4^{-1}$: –4.5‰; $LSU\text{-}BaSO_4^{-2}$: +38.5‰; Meng et al., 2019).

RESULTS AND DISCUSSION

Ratios of sulphur isotopes are shown in per mil (‰) relative to the sulphur isotope composition of the standard *Vienna-Canyon Diablo Troilite* (V-CDT) using $\delta^{34}S$ notation. Sulphur isotope data for sulphate-bearing evaporites from the Salt Range Formation ranged from +32.1 to +37.6‰ (mean = +33.6‰, n = 8) from the first section (Table 1), and ranged from +29.6 to +34.4‰ (mean = +34.0‰, n = 27) from the second section (Table 2).

Sulphur isotope values ($\delta^{34}S$) for middle Proterozoic evaporite deposits are generally below +20‰ (from +10 to +18‰) (Strauss, 1993) and gradually increase to their maximum within postglacial Neoproterozoic and Cambrian deposits (Strauss et al., 2001; Shields et al., 2004; Schröder et al., 2004, 2008; Halverson and Hurtgen, 2007; Shields and Mills, 2019; Meng et al., 2019; Present et al., 2020).

Holser (1977) termed this upward increase in strongly positive $\delta^{34}S$ values (+30 to +35‰, and sometimes up to 45‰) as the "Yudomski Event" (~575 Ma) for the upper Neoproterozoic-Cambrian evaporites in SE Siberia. The "Yudomski Event" has been reported from the Neoproterozoic–lower Cambrian evaporites of southeastern Siberia in Russia, as well as from the Hormuz Formation and Desu Series in Iran, the Hanseran Formation in India, and the Wusonggeer Formation in the Tarim Basin, northwestern China (Holser, 1977; Claypool et al., 1980; Houghton, 1980; Strauss et al., 2001; Peryt et al., 2005; Meng et al., 2019). Additionally, positive $\delta^{34}S$ phosphorite signatures and those in structurally bound sulphate-bearing carbonates (by using structurally substituted sulphate present in phosphorite and micritic carbonates) in Neoproterozoic–lower Cambrian deposits have been reported in many studies (Shields et al., 1999; Mazumdar et al., 2008; Tostevin et al., 2017; He et al., 2019). For example, Shields et al. (1999) reported large positive

Table 2

Gypsum samples were collected from the second section through the Salt Range Formation (Bhandar Kas Gypsum/Sahwal Marl) and their sulphur isotope data in this study

Samples (from top to base)	Lithology	$\delta^{34}S$ [‰]	Member
KSR-102	pure white gypsum	29.6	Sahwal Marl
KSR-93	pure white gypsum	30.5	Sahwal Marl
KSR-90	pure white gypsum	30.3	Sahwal Marl
KSR-86	pure white gypsum	30.6	Sahwal Marl
KSR-82	pure white gypsum	30.5	Sahwal Marl
KSR-79	pure white gypsum	30.9	Sahwal Marl
KSR-67	pure white gypsum	31.2	Sahwal Marl
KSR-66	pure white gypsum	31.4	Sahwal Marl
KSR-65	pure white gypsum	34.4	Sahwal Marl
KSR-61	pure white gypsum	36.3	Sahwal Marl
KSR-60	pure white gypsum	36.4	Sahwal Marl
KSR-59	pure white gypsum	36.0	Sahwal Marl
KSR-58	pure white gypsum	36.0	Sahwal Marl
KSR-57	pure white gypsum	35.5	Sahwal Marl
KSR-55	pure white gypsum	36.3	Sahwal Marl
KSR-53	pure white gypsum	35.5	Bhandar Kas Gypsum
KSR-52	pure white gypsum	35.1	Bhandar Kas Gypsum
KSR-51	pure white gypsum	36.4	Bhandar Kas Gypsum
KSR-50	pure white gypsum	34.6	Bhandar Kas Gypsum
KSR-47	pure white gypsum	35.6	Bhandar Kas Gypsum
KSR-45	pure white gypsum	35.6	Bhandar Kas Gypsum
KSR-43	pure white gypsum	35.8	Bhandar Kas Gypsum
KSR-42	pure white gypsum	34.0	Bhandar Kas Gypsum
KSR-33	pure white gypsum	35.6	Bhandar Kas Gypsum
KSR-31	pure white gypsum	34.9	Bhandar Kas Gypsum
KSR-25	pure white gypsum	32.9	Bhandar Kas Gypsum
KSR-24	pure white gypsum	35.1	Bhandar Kas Gypsum

All data ranged from +29.6 to +37.6‰ (mean = +33.9‰, n = 35; Fig. 4)

$\delta^{34}S$ values (+29–37‰, avg. = +33 ±2‰, n = 40) from forty phosphorite samples collected from a Precambrian–Cambrian Meishucun exposure on the Yangtze Platform in China. Similarly, structurally substituted sulphate present in Ediacaran and Cambrian micritic carbonates on the Yangtze Block have yielded strongly positive $\delta^{34}S$ values (Zhang et al., 2003, 2004). The "Yudomski Event" has been placed in the framework of a model of a possible "Snowball Earth" and associated oxidation of the Ediacaran Ocean (Strauss et al., 2001; Fike et al., 2006).

The enrichment signature of $\delta^{34}S$ in chemical deposits across the Precambrian-Cambrian boundary is well-established, but its ultimate cause is still a matter of debate (Warren, 2016). Holser (1977, 1984) suggested that bacterial sulphides accumulated in relatively deep parts of rift basins under a reducing environment. Sulphate reduction then resulted in the removal of ^{32}S and enrichment of ^{34}S in brines, producing strongly positive sulphur isotope values. Upwelling currents carried ^{34}S-rich brines toward shallow seas, and they mixed with surface seawaters at the end of the glacial period. Gorjan et al. (2000), Hurtgen et al. (2002), and Zhang et al. (2003) also supported this model for the strongly positive ^{34}S values of Neoproterozoic deposits in Australia, Namibia, and China (Doushantuo Formation). The onset and termination of the global snowball glaciations can account for the rapid transfer of ^{34}S-rich brines toward shallow seas and enrich sulphate deposits in ^{34}S worldwide after the Neoproterozoic glaciations (Hoffman et al., 1998; Strauss et al., 2001; Meng et al., 2019).

Previous studies have demonstrated that sulphur isotope data vary widely within marine evaporites throughout geological history (Fig. 5). This variability depends upon the influx of river sulphate, mainly derived from the continental weathering of sulphates and sulphides. Modern rivers have a globally average $\delta^{34}S$ = +8‰ (Grinenko and Krouse, 1992) or 4.4 ±4.5‰ (Burke et al., 2018) where the sulphur isotopic composition depends on the geology of (and thus yielding dissolved SO_4^{-2} to) the river basin. Additionally, the presence of sulphate-reducing bacteria in depositional basins can lead to irregular isotopic values during the precipitation of sulphate minerals, driven by enhanced primary production and sequestration of organic carbon (e.g., Bottrell and Newton, 2005; Fike and Grotzinger, 2008; Cui et al., 2015; Och et al., 2016).

A strong positive shift of ^{34}S values within an evaporite sequence may result from closed system conditions and/or a limited sulphate supply (Strauss, 1993; Li et al., 2018). Both effects become vital in the case of evaporite basins that are partially separated from the open ocean. Data acquired from such basins have broad regional importance rather than global implications. By contrast, huge evaporite basins may have records of

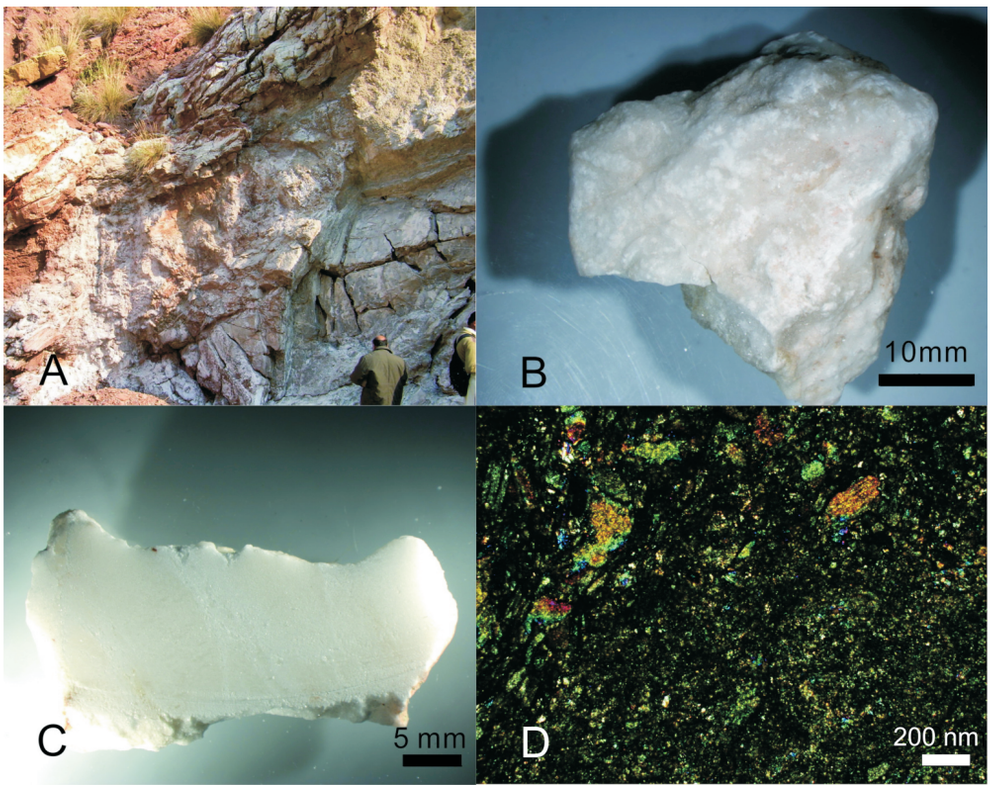

Fig. 3A – exposure of white to dirty white gypsum in the Bandar Kas Gypsum Member of the Salt Range Formation, on the right bank of the Khewra Gorge, Eastern Salt Range; dull red marls overlie the massively bedded gypsum beds; B – hand specimen of massive white gypsum of the Bhandar Kas Gypsum Member derived from the exposure shown in the photo (A); C – polished section of the massive white gypsum (B) indicates that it is devoid of impurities; D – microphotograph of sample (B), under CNL, shows very finely crystalline gypsum with some large elongated and acicular crystals of gypsum and platy to prismatic anhydrite

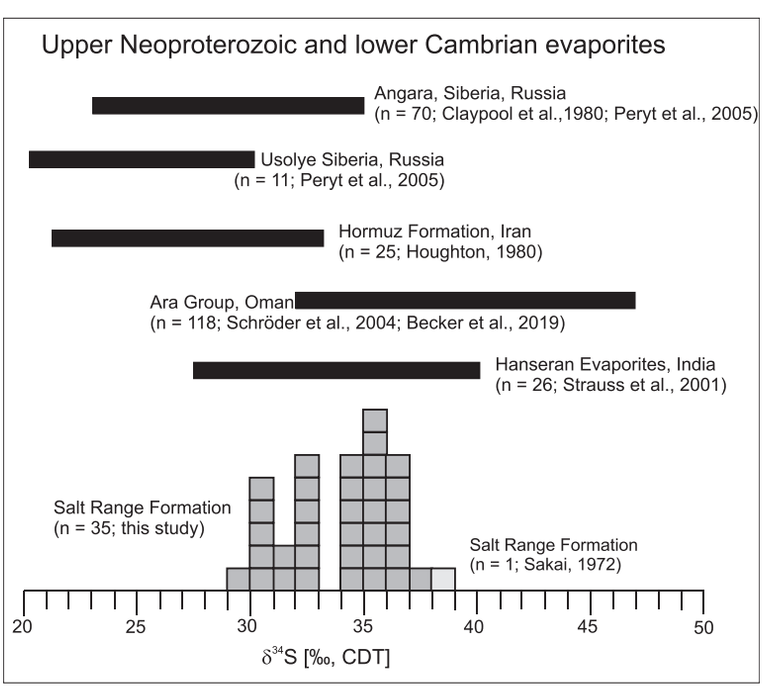

Fig. 4. Sulphur isotopic composition of evaporites from the Salt Range Formation compared to previous data

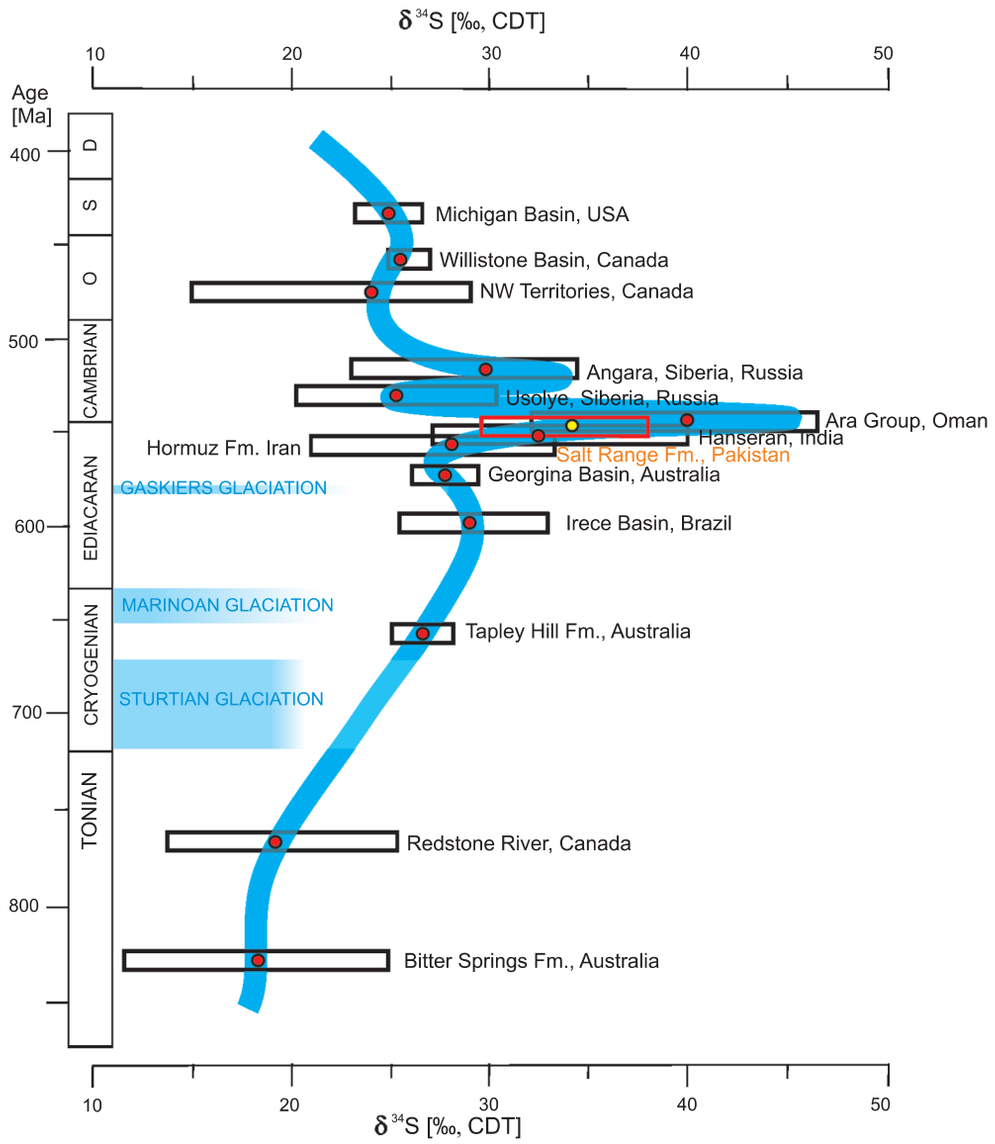

Fig. 5. Temporal evolution of $\delta^{34}S$ during end-Neoproterozoic and early Paleozoic times (after Strauss and Banerjee, 1998; Hough et al., 2006), using evaporite sulphate data from the literature (Holser and Kaplan, 1966; Claypool et al., 1980; Houghton, 1980; Strauss, 1993; Fox and Videtich, 1997; Misi and Veizer, 1998; Gorjan et al., 2000; Schröder et al., 2004; Hurtgen et al., 2005; Peryt et al., 2005; Hough et al., 2006; Tostevin et al., 2017; He et al., 2019; Becker et al., 2019) and this study – Salt Range Formation, Pakistan, box dimensions range represent entire data, and red circles show mean values

global importance (Fig. 5; Strauss et al., 2001; Fike et al., 2006; Tostevin et al., 2017; He et al., 2019; Present et al., 2020). Similarly, the sulphate isotopes of modern seawater are very stable between +20 and +20.5‰ (Longinelli, 1989). Yet, this can vary in some semi-closed basins; for instance, the Black Sea water's sulphur isotope values are between +18.20 and +20.17‰ due to riverine influx (Sweeney and Kaplan, 1980).

Suppose a marine evaporite basin is affected by a large amount of river input. In that case, its sulphur isotope will be significantly reduced because the average value of the sulphur isotope of the modern river is only +8% (Grinenko and Krouse, 1992). On the other hand, if a marine evaporite basin is frequently recharged by seawater, its sulphur isotope composition tends to be close to that of seawater (Li et al., 2018).

Suppose brine stratification occurs in an evaporite basin. In that case, the residual sulphate in the lower brine layer will become heavier due to the reduction of sulphate by bacteria, making the sulphur isotope value of gypsum reach a very high value. This has been observed in saline continental basins in China, such as the continental evaporites in the Qianjiang depression, Jianghan Basin. These evaporites have high $\delta^{34}S$ values from +31 to +40.43‰. The continental evaporites in the Dongpu Dof Bohai Bay Basin also have high $\delta^{34}S$ values from +28 to +33‰ (Li et al., 2018). These gypsum deposits are usually interbedded with black shales, indicating an anoxic sedimentary environment. This kind of environment may be caused by brine stratification in a deep basin (Gao et al., 2009).

Table 3

Regional Correlation of Neoproterozoic–lower Cambrian Sequence of Yangtze Platform in China, N.W. India and Salt Range Formation in Pakistan

Age	Yangtze Block, Sichuan Province, China (after Meng et al., 2011a)	Yangtze Block, Hubei Province, Yichang City, China (after Zhang et al., 2004)	N.W. India (after Peters et al., 1995)	Salt Range Pakistan (after Shah, 1977, 2009)
lower Cambrian	**Jiulaodong Formation (Qiongzhusi Formation)** The lower part comprises black shale. Its contact is disconform able on the lower. Maidiping Formation; the thickness is ~850 m **Maidiping Formation** Carbonaceous chert interbedded with dolomite and shale. The thickness is ~1000 m	**Tianzhushan Section** The top consists of phosphoric dolomite with small shell fossils. In places, it contains phosphate rock. Its thickness varies from 1 to 5 m	**Nagur Formation** Sandstone and shales with siltstones	**Baghanwala Formation** Red shales and clay with flaggy sandstone **Jutana Formation** Light green, sandy dolomite **Kussak Formation** Sandstone, red flaggy shales in the lower parts, greenish-grey glauconitic sandstone **Khewra Sandstone** Purple to brown sandstone lowermost part contains flaggy shale Oil shales at the top of Salt Range Formation
Ediacaran	**Hongchunping Formation** (thickness is ~1000 m) **Upper Section** The upper part is mainly composed of dolomite **Lower Section** Composed of dolomite and halite. The dolomite contains anhydrite. Halite top is composed of glauberite. Chert at the base	**Dengying Formation** (thickness is 200–1000 m) **Baimatuo Member** The upper part is mainly grey siliceous dolomite, dolomicrite, crystalline dolomite, and intraclastic dolomite interlayered with chert beds, nodules, and autobreccia **Shibantan Member** The middle part is black siliceous and bituminous micrite with gypsum beds **Hamajing Member** The lower part contains intraclastic dolomite with oncolites, chert, and nodules	**Hanseran Formation** Siltstone, sandstone, claystone, and evaporites **Bilara Formation** Dolomite and limestone **Jodhpur Formation** Sandstone, siltstone, shales, clays, and dolomitic limestone	**Salt Range Formation** (thickness is 800 m) **Sahwal Marl Member** Bright red marl, gypsum, dolomite, chert, and Khewra Trap Dull red marl with salt, a 10 m thick bed of gypsum occurs at the top **Bhandar Kas Gypsum Member** Massive gypsum with dolomites and clays, >80 m thick **Billianwala Salt Marl Member** Red marl with salt, >650 m thick
	Labagang Formation This formation is not fully drilled. The upper part is mainly composed of sandstone, and the lower part contains mudstone Its thickness is >300 m	**Doushantuo Formation** Composed of dolomite with interbedded black shales. Its thickness is from 100 to 230 m	**Basement Rocks**	**Basement Rocks**
	Metamorphic basement	**Nantuo Formation** Tillite and diamictites		

Strongly positive $\delta^{34}S$ values can be observed in late Ediacaran-early Cambrian marine evaporites of India, Iran, Oman and the Tarim Basin in China (Strauss et al., 2001; Schröder et al., 2004, 2008; Halverson and Hurtgen, 2007; Shields and Mills, 2019; Meng et al., 2019). These high $\delta^{34}S$ values in different regions of the same geological age indicate that the ocean had very high sulphur isotope background levels at that time (Strauss et al., 2001). The gypsum deposits in the Salt Range Formation are usually interbedded with red marls (Kadri, 1995; Ahsan et al., 2013), indicating an oxidized shallow water environment. The brine was not stratified, and the original sulphur isotope information of brine from seawater can be directly recorded.

In addition to the Salt Range Formation results of this study, strongly positive $\delta^{34}S$ data (+30.2 to +34.8‰; n = 11) have also been reported for the lower–middle Cambrian evaporites of the Tarim Basin (Meng et al., 2019). These data indicate that seawater with a strongly positive sulphur isotope ratio within sulphate continued to prevail from the Late Neoproterozoic to the middle Cambrian (Fig. 5).

REGIONAL CORRELATION OF PROTEROZOIC – LOWER CAMBRIAN FORMATIONS

The Salt Range Formation is lithologically comparable to rocks of the terminal Neoproterozoic to lower Cambrian of northwestern India and the Ediacaran of the Yangtze Block in South China (Jones, 1970). Neoproterozoic stratigraphic comparison between India and the Yangtze Block also reveals obvious similarities (Jiang et al., 2003). Zhang et al. (2003, 2004) and Meng et al. (2011a) developed useful chronostratigraphic frameworks (Table 3). However, a comprehensive stratigraphic and chemostratigraphic correlation between the Neoproterozoic of Indo-Pakistan and China remains lacking. Sparse palaeomagnetic data and similar sedimentary assemblages indicate that the Yangtze Block of South China was located to the north-west of India and Pakistan (Jiang et al., 2003; Allen, 2007; Fig. 2) when the evaporitic belt formed during the terminal Neoproterozoic (Husseini and Husseini, 1990).

The upper Ediacaran Dengying Formation (551–541 Ma) is well-exposed in the Three Gorges area near Yichang city in southern China. From the base to the top, this formation (Table 3) can be divided into three members: the Hamajing, Shibantan, and Baimatuo (Zhao et al., 1980). The Hamajing Member contains grey intraclastic dolomite with oncolites, chert beds, and nodules. The Shibantan Member is composed of a thin black layer of siliceous and asphaltene-rich finely crystalline limestone with high organic matter content. Abundant macroalgae, organic-walled microfossils, and trace fossils have been found in this section. Finally, the Baimatuo Member consists of grey and greyish-purple layered silico-phosphatic dolomites and chert (Zhao et al., 1980).

The Hongchunping Formation, located on the Yangtze Block (Table 3) in South China and represented in the Changning-2 borehole, is lithologically divisible into two sections (Meng et al., 2011a). The lower section (2492.5–2992.5 m in depth) is mainly composed of dolomite, anhydrite, and halite, while the upper section (1975–2492.5 m in depth) comprises dolomite and grapestone-bearing dolomite. Moreover, the Hongchunping Formation is overlain by the Lower Cambrian Maidiping Formation which contains abundant small shelly fossils and is composed of carbonaceous chert interbedded with dolomite and black shale (Meng et al., 2011a). Previously, strongly positive $\delta^{34}S$ values (+29 to +37‰; avg. = +33 ±2‰; n = 40) were reported from phosphorite samples from an exposure of the lower Cambrian Meishucun section on the Yangtze Platform in China (Shields et al., 1999).

In northwestern India, the Hanseran Formation (Table 3), equivalent to the Salt Range Formation, is present within a subsurface Neoproterozoic-early Cambrian evaporite basin. This formation records seven halite cycles interbedded with marls and stromatolitic carbonates (Dey, 1991; Banerjee et al., 1998). These evaporites are mainly composed of anhydrite and halite and possess strongly positive $\delta^{34}S$ signatures, ranging from +27.5 to +35.6‰ (Strauss and Banerjee, 1998). Strauss et al. (2001) also reported strongly positive sulphur isotope data (+27.5 to +39.7‰) from the Hanseran evaporites.

Both the Dengying and Hanseran formations in China and India can be correlated with the Salt Range Formation based on their stratigraphic position, lithology, age, and sulphur isotope data. For example, gypsum is present in the middle of both the Dengying (Zhao et al., 1980) and the Salt Range formations (Bhandar Kas Gypsum Member). Moreover, the Dengying Formation in the Three Gorges area near Yichang can be correlated lithologically with the Hongchunping Formation near Changning in Sichuan Province (Zhang et al., 2004; Meng et al., 2011a). Similarly, the Lower Billianwala Salt Member of the Salt Range Formation and the Lower Hongchunping Formation contain halite deposits. This lithological similarity suggests that the Billianwala Salt Member can be correlated with the Lower Hongchunping Formation in South China. Oil shales with highly altered volcanic rocks (Khewra Trap) outcrop at the top of the Salt Range Formation, while carbonaceous cherts interbedded with dolomite and black shale are associated with the lower Cambrian Maidiping Formation on the Yangtze Block, which suggests that there is a correlation between the Maidiping Formation and the top of the Salt Range Formation (Zhang et al., 2004; Meng et al., 2011a).

Fan et al. (2013) correlated the presence of cherts on the Yangtze Block with hydrothermal activity. A layer of volcanic rock attributed to the Khewra Trap can be found at the top of the Salt Range Formation (Shah, 2009). Additionally, the evaporites of the Salt Range Formation may be correlated with those of the Hanseran Formation (Dasgupta and Bulgauda, 1994; Peters et al., 1995). From their similar stratigraphic details, including lithologies, unconformities, and range of intertidal-supratidal-basinal facies architecture in a rifted margin (Husseini and Husseini, 1990; Peters et al., 1995), it can be inferred that the Yangtze Block in China and the Salt Range in northwestern India were closely related palaeogeographically during the Neoproterozoic–early Cambrian (Jiang et al., 2003).

Moreover, organic geochemical analyses of hydrocarbons from the Baghewala-1 oil trapped in the Hanseran Evaporite Group of India revealed similarities between these oils and the oil-bearing successions in Huqf, Oman, and Karampura, Pakistan (Peters et al., 1995). These organic geochemical similarities of oils originating from terminal Neoproterozoic-early Cambrian strata imply close relationships among the evaporite belts in Oman, Pakistan, and India (Peters et al., 1995). The organic carbon isotope data for the Baghewala-II borehole range from –37.1 to –33.0‰ (Table 4). The $\delta^{13}C_{org}$ data from source rocks tend to be heavier from lower to upper (Mazumdar and Bhattacharya, 2004).

The organic carbon isotopic patterns of the Baghewala-II well show similar numerical ranges with those of the contemporaneous oil and hydrocarbon source rocks in Pakistan, India,

Table 4

Organic carbon isotope ratios in oil from Pakistan compared to other oils, source rock extracts, and kerogen from India and Oman

Borehole	Location	$\delta^{13}C_{org}$ [‰]	Type of samples
Karampur-1	Pakistan	–37.0	tar
Baghewala-1	India	–32.4	oil
Baghewala-II	India (484.42 m in depth)	–33.0	kerogen
Baghewala-II	India (484.63 m in depth)	–33.6	kerogen
Baghewala-II	India (513.49 m in depth)	–36.9	kerogen
Baghewala-II	India (517.45 m in depth)	–37.1	kerogen
Baghewala-II	India (518.27 m in depth)	–37.0	kerogen
Baghewala-II	India (519.31 m in depth)	–37.1	kerogen
Baghewala-II	India (521.8 m in depth)	–36.5	kerogen
Baghewala-II	India (522.08 m in depth)	–37.1	kerogen
Baghewala-II	India (523.35 m in depth)	–36.9	kerogen
Baghewala-II	India (548.8 m in depth)	–37.1	kerogen
Baghewala-II	India (550.5 m in depth)	–35.8	kerogen
Baghewala-II	India (551.705 m in depth)	–35.5	kerogen
Baghewala-II	India (552.375 m in depth)	–37.1	kerogen
Baghewala-II	India (553.26 m in depth)	–36.7	kerogen
Amal S-1	Oman (Huqf oil)	–35.9	oil
Nuham-1	Oman (Huqf oil)	–37.2	oil
Rima-7	Oman (Huqf oil)	–36.2	oil
Runib-1	Oman (Huqf oil)	–36.5	oil
Amal-9 rock	Oman (Huqf rock)	–34.7	source rock
Nimr-4 rock	Oman (Huqf rock)	–35.4	source rock
Runib-1 rock	Oman (Huqf rock)	–35.2	source rock
Sayyala-1	Oman ('Q' oils)	–30.3	oil
Bahja-1	Oman ('Q' oils)	–30.4	oil
Bahja-1	Oman ('Q' oils)	–30.9	oil
Zareef-1	Oman ('Q' oils)	–31.0	oil

Oman (Huqf oil) come from Huqf Group, and Oman ('Q' oils) come from early Cambrian source rocks; Pakistan and Oman data from Grantham et al. (1990), Baghewala-1 data from Peters et al. (1995); Baghewala-II data from Mazumdar and Bhattacharya (2004)

and Oman, suggesting that they came from similar sedimentary environments (Peters et al., 1995; Mazumdar and Bhattacharya, 2004). The Oman oils also show that $^{13}C_{org}$ values tend to be heavier from lower to upper. The Huqf oil of Oman comes from the upper Neoproterozoic-lower Cambrian Huqf Group and show the heavier organic carbon isotope ratio. Oils come from younger early Cambrian source rocks ('Q' oils) show the lighter organic carbon isotope signature (Grantham et al., 1990; Grosjean et al., 2012; Table 4).

Organic geochemical signatures can provide clear evidence for correlating stratigraphic units across large areas. For example, the similarities of oils and source rocks between basins in West Africa and Brazil (now ~6000 km apart) provide evidence for the opening of the Atlantic Ocean during the Cretaceous (Mello et al., 1991). The organic geochemical characteristics of oils and solid asphalts from Oman, India, Pakistan, and the Sichuan Basin of South China show strong similarities, implying that they are related in terms of genesis and host rocks (Wang et al., 2015).

CONCLUSIONS

The strongly positive sulphur isotopic data from the gypsum of the Salt Range Formation (+29.6 to +37.6‰; mean = +33.9‰, n = 35) reported in this study are similar to those of terminal Neoproterozoic and early Cambrian evaporites on the Yangtze Platform, China, and NW India. New data supports the regional distribution of the event. However, there are limitations when considering the use of evaporite records for stratigraphy (e.g., records of $\delta^{34}S$ from evaporites are stratigraphically intermittent, and the spread of $\delta^{34}S$ data over each time interval is very large, making direct stratigraphic correlations difficult; Yao et al., 2019). Despite that, based on their stratigraphic and organic geochemical similarities, it may be inferred that the late Neoproterozoic Indo-Pakistan Plate and Yangtze Platform were geographically adjacent. This study also shows that the stratigraphic position of evaporites in northern Pakistan is similar to that in South China, during the late Neoproterozoic-early Cambrian. This relationship should be accounted for in future studies on the geological evolution of South China and Indo-Pakistan.

Acknowledgments. We sincerely appreciate G. Shields (University College London), A. Mazumdar (National Institute of Oceanography, India) and an anonymous reviewer for all the valuable comments that helped us improve the article's quality. This work was financially supported by the National Natural Science Foundation of China (grant no. 41672142 and 41561144009), the Basic Frontier Scientific Research Program of the Chinese Academy of Sciences (grant no. ZDBS-LY-DQC021), AGH University of Science and Technology (grant no 16.16.140.315 for KB) and by the Bureau of International Co-operation, Chinese Academy of Sciences.

REFERENCES

Ahmad, W., Alam, S., 2007. Organic geochemistry and source rock characteristics of Salt Range Formation, Potwar Basin, Pakistan. Journal of Hydrocarbon Research, **17**: 37–59.

Ahsan, N., Mairaj, F.A., Rehman, S.U., Ali, A., 2013. Subsurface structural reconstruction of Joya Mair structure, southeast Potwar sub-basin, Pakistan. International Journal of Agriculture and Applied Sciences, **5**: 17–26.

Alavi, M., 2004. Regional stratigraphy of the Zagros fold-thrust belt of Iran and its proforeland evolution. American Journal of Science, **304**: 1–20.

Allen, P.A., 2007. The Huqf Supergroup of Oman: basin development and context for Neoproterozoic glaciation. Earth-Science Reviews, **84**: 139–185.

Asrarullah, P., 1967. Geology of the Khewra Dome. Proceedings of the 18th and 19th combined session of All Pakistan Science Conference, University of Sind, Hyderabad, Part–III, Abstracts, F3–F4.

Banerjee, D.M., Strauss, H., Bhattacharya, S.K., Kumar, V., Mazumdar, A., 1998. Isotopic composition of carbonate and sulphates, potash mineralisation and basin architecture of the Nagaur-Ganganagar evaporate basin (northwestern India) and their implications on the Neoproterozoic exogenic cycle. Mineralogical Magazine, **62A**: 106–107.

Becker, S., Reuning, L., Amthor, J.E., Kukla, P.A., 2019. Diagenetic processes and reservoir heterogeneity in salt-encased microbial carbonate reservoirs (Late Neoproterozoic, Oman). Geofluids, Article ID 5647857. https://doi.org/10.1155/2019/5647857

Benison, K.C., 1995. Surface water paleotemperatures from Permian Nippewalla Group halite, Kansas. Carbonates and Evaporites, **10**: 242–248.

Bottrell, S.H., Newton, R.J., 2005. Reconstruction of changes in global sulfur cycling from marine sulfate isotopes. Earth-Science Reviews, **75**: 59–83.

Bukowski, K., Galamay, A.R., Góralski, M., 2000. Inclusion brine chemistry of the Badenian salt from Wieliczka. Journal of Geochemical Exploration, **69–70**: 87–90.

Bukowski, K., Czapowski, G., Karoli, S., Bąbel, M., 2007. Sedimentology and geochemistry of the Middle Miocene (Badenian) salt-bearing succession from East Slovakian Basin (Zbudza Formation). Geological Society, Special Publication, **285**: 247–264.

Burke, A., Present, T.M., Paris, G., Rae, E., Sandilands, G.H., Gaillardet, J., Peucker-Ehrenbrink, B., Fischer, W.W., McClelland, J.W., Spencer, R., Voss, B., Adkins, J.F., 2018. Sulfur isotopes in rivers: insights into global weathering budgets, pyrite oxidation, and the modern sulfur cycle. Earth and Planetary Science Letters, **496**: 168–177.

Chaudhuri, S., Clauer, N., 1992. History of marine evaporites: constraints from radiogenic isotopes. Lecture Notes in Earth Sciences, **43**: 177–198.

Chen, C.X., Ni, P., Cai, K.Q., Zhai, Y.S., Deng, J., 2003. The minerogenic fluids of magnesite and talc deposits in the Paleoproterozoic Mg-rich carbonate formations in Eastern Liaoning Province (in Chinese with English summary). Geological Reviewer, **49**: 646–651

Claypool, G.E., Holser, W.T., Kaplan, I.R., Sakai, H., Zak, I., 1980. The age curves of sulfur and oxygen isotopes in marine sulfate and their mutual interpretation. Chemical Geology, **28**: 190–260.

Craig, J., Thurow, J., Thusu, B., Whitham, A., Abutarruma, Y., 2009. Global Neoproterozoic petroleum systems: the emerging potential in North Africa. Geological Society Special Publications, **326**: 1–25.

Cui, H., Kaufman, A.J., Xiao, S., Zhu, M., Zhou, C., Liu, X.M., 2015. Redox architecture of an Ediacaran ocean margin: integrated chemostratigraphic ($\delta^{13}C$–$\delta^{34}S$–$^{87}Sr/^{86}Sr$–Ce/Ce*) correlation of the Doushantuo Formation, South China. Chemical Geology, **405**: 4–62.

Cui, H., Kaufman, A.J., Xiao, S.H., Peek, S., Cao, H.S., Min, X., Cai, Y.P., Siegel, Z., Liu, X.M., Peng, Y.B., 2016. Environmental context for the terminal Ediacaran biomineralization of animals. Geobiology, **14**: 344–363.

Dasgupta, U., Bulgauda, S.S., 1994. An overview of the geology and hydrocarbon occurrences in the western part of Bikaner-Nagaur Basin. Indian Journal of Petroleum Geology, **3**: 1–17.

Dey, R.C., 1991. Trans-Aravalli Vindhyan evaporites under the semi-desertic plains of Western India-significance of depositional features. Journal of the Geological Society of India, **37**: 136–150.

Dong, A., Zhu, X.K., Li, S.Z., Kendall, B., Wang, Y., Gao, Z., 2016. Genesis of a giant Paleoproterozoic strata-bound magnesite deposit: constraints from Mg isotopes. Precambrian Research, **281**: 673–683.

Fan, H.F., Wen, H.J., Zhu, X.K., Hu, R.Z., Tian, S.H., 2013. Hydrothermal activity during Ediacaran–Cambrian transition: silicon isotopic evidence. Precambrian Research, **224**: 23–35.

Faramarzi, N.S., Amini, S., Schmitt, A.K., Hassanzadeh, J., Borg, G., Mckeegan, K., Mortazavi, S.M., 2015. Geochronology and geochemistry of rhyolites from Hormuz Island, southern Iran: a new record of Cadomian arc magmatism in the Hormuz Formation. Lithos, **236**: 203–211.

Fatmi, A.N., 1973. Lithostratigraphic units of the Kohat-Potwar Province, Indus Basin. Geological Survey of Pakistan Memoirs, **10**: 1–80.

Fike, D.A., Grotzinger, J.P., 2008. A paired sulfate-pyrite delta S-34 approach to understanding the evolution of the Ediacaran-Cambrian sulfur cycle. Geochimica et Cosmochimica Acta, **72**: 2636–2648.

Fike, D.A., Grotzinger, J.P., Pratt, L.M., Summons, R.E., 2006. Oxidation of the Ediacaran Ocean. Nature, **444**: 744–747.

Fox, J.S., Videtich, P.E., 1997. Revised estimate of $\delta^{34}S$ for marine sulfates from the Upper Ordovician: data from the Williston Basin, North Dakota, USA. Applied Geochemistry, **12**: 97–103.

Galamay, A.R., Bukowski, K., Czapowski, G., 2003. Chemical composition of brine inclusions in halite from clayey salt (zuber) facies from the Upper Tertiary (Miocene) evaporite basin (Poland). Journal of Geochemical Exploration, **78–79**: 509–511.

Galamay, A.R., Bukowski, K., Sydor, D.V., Meng, F., 2020. The ultramicrochemical analyses (UMCA) of fluid inclusions in halite and experimental research to improve the accuracy of measurement. Minerals, **10**: 823.

Gao, H.C., Chen, F.L., Zhao, G.R., Liu, Z.F., 2009. Advances, problems and prospect in studies of origin of salt rocks of the Paleogene Shahejie Formation in Dongpu Sag (in Chinese with English summary). Journal of Palaeogeography, **11**: 251–264.

Gee, E.R., 1945. The age of saline series of Punjab and Kohat. Proceedings of the National Academy of Sciences, India **14**, Part 6: 269–310.

Gorjan, P., Veevers, J.J., Walter, M.R., 2000. Neoproterozoic sulfur-isotope variation in Australia and global implications. Precambrian Research, **100**: 151–179.

Grantham, P.J., Lijmbach, G.W.M., Posthuma, J., 1990. Geochemistry of crude oils in Oman. Geological Society Special Publications, **50**: 317–328.

Grelaud, S., Sassi, W., de Lamotte, D.F., Jaswal, T., Roure, F., 2002. Kinematics of eastern Salt Range and South Potwar Basin (Pakistan): a new scenario. Marine and Petroleum Geology, **19:** 1127–1139.

Grinenko, V.A., Krouse, H.R., 1992. Isotope data on the nature of riverine sulfates. Mitteilungen Geologisch-Paläontologisches Institut der Universität Hamburg, **72**: 9–18.

Grosjean, E., Love, G.D., Kelly, A.E., Taylor, P.N., Summons, R.E., 2012. Geochemical evidence for an Early Cambrian origin of the 'Q' oils and some condensates from north Oman. Organic Geochemistry, **45**: 77–90.

Halverson, G.P., Hurtgen, M.T., 2007. Ediacaran growth of the marine sulfate reservoir. Earth and Planetary Science Letters, **263**: 32–44.

Hałas, S., Szaran, J., 1999. Low-temperature thermal decomposition of sulfate to SO_2 for on-line $^{34}S/^{32}S$ analysis. Analytical Chemistry, **77**: 3254–3257.

He, T., Zhu, M., Mills, B.J.W., Wynn, P.M., Zhuravlev, A.Y., Tostevin, R., Pogge von Strandmann, P.A.E., Yang, A., Poulton, S.W., Shields, G.A., 2019. Possible links between extreme oxygen perturbations and the Cambrian radiation of animals. Nature Geoscience, **12**: 468–474.

Hoefs, J., 2004. Stable Isotope Geochemistry (5th edition). Springer, Berlin.

Hoffman, P.F., Kaufman, A.J., Halverson, G.P., Schrag, D.P., 1998. A Neoproterozoic Snowball Earth. Science, **281**: 1342–1346.

Holser, W.T., 1977. Catastrophic chemical events in the history of the ocean. Nature, **267**: 403–408.

Holser, W.T., 1984. Gradual and abrupt shifts in ocean chemistry during Phanerozoic time. In: Patterns of Change in Earth Evolution (eds. H.D. Holland and A.F. Trendall): 123–143. Springer-Verlag, Berlin.

Holser, W.T., Kaplan, I.R., 1966. Isotope geochemistry of sedimentary sulfates. Chemical Geology, **1**: 93–135.

Holser, W.T., Schidlowski, M., Mackenzie, F.T., Maynard, J.B., 1988. Geochemical cycles of carbon and sulfur. In: Chemical Cycles in the Evolution of the Earth (eds. C.B. Gregor, R.M. Garrels, F.T. Mackenzie and J.B. Maynard): 107–173. Wiley, New York.

Hough, M.L., Shields, G.A., Evins, L.Z., Strauss, H., Henderson, R.A., Mackenzie, S., 2006. A major sulphur isotope event at c. 510 Ma: a possible anoxia–extinction volcanism connection during the Early-Middle Cambrian transition? Terra Nova, **18**: 257–263.

Houghton, M.L., 1980. Geochemistry of the Proterozoic Hormuz Evaporites, Southern Iran. M.Sc. Thesis, University of Oregon.

Hurtgen, M.T., Arthur, M.A., Suits, N.S., Kaufman, A.J., 2002. The sulfur isotopic composition of Neoproterozoic seawater sulfate: implications for a snowball Earth? Earth and Planetary Science Letters, **203**: 413–429.

Hurtgen, M.T.,Arthur, M.A., Halverson, G.P., 2005. Neoproterozoic sulfur isotopes, the evolution of microbial sulfur species, and the burial efficience of sulfide as sedimentary pyrite. Geology, **33**: 41–44.

Hussain, S.A., Han, F.Q., Han, J., Khan, H., Widory, D., 2020. Chlorine isotopes unravel conditions of formation of the Neoproterozoic rock salts from the Salt Range Formation, Pakistan. Canadian Journal of Earth Science, **57**: 698–708.

Hussain, S.A., Han, F.-Q., Ma, Z., Hussain, A., Mughal, M.S., Han, J., Alhassan, A., Widory, D., 2021. Unraveling sources and climate conditions prevailing during the deposition of Neoproterozoic evaporites using coupled chemistry and Boron isotope compositions ($\delta^{11}B$): the example of the Salt Range, Punjab, Pakistan. Minerals, **11**: 161.

Husseini, M.I., Husseini, S.I., 1990. Origin of the Infracambrian Salt Basins of the Middle East. Geological Society Special Publications, **50**: 279–292.

Jaworska, J., Wilkosz, P., 2012. An oxygen and sulfur isotopic study of gypsum from the Mogilno Salt Dome cap-rock (Poland). Geological Quarterly, **56**: 249–250.

Jiang, G., Sohl, L.E., Christie-Blick, N., 2003. Neoproterozoic stratigraphic comparison of the Lesser Himalaya (India) and Yangtze block (south China): paleogeographic implications. Geology, **31**: 917–920.

Jones, C.L., 1970. Potash in halitic evaporite salt, western Pakistan. United States Department of the Interior, U.S. Geological Survey Professional Paper, **770 D**: 140–145.

Kadri, I.B., 1995. Petroleum Geology of Pakistan. Pakistan Petroleum Limited Publication: 136–142.

Kampschulte, A., Strauss, H., 2004. The sulfur isotopic evolution of Phanerozoic seawater based on the analysis of structurally substituted sulfate in carbonates. Chemical Geology, **204**: 255–286.

Khan, I., Zhong, N., Luo, Q., Ai, J., Yao, L., Luo, P., 2020. Maceral composition and origin of organic matter input in Neoproterozoic–Lower Cambrian organic-rich shales of Salt Range Formation, upper Indus Basin, Pakistan. International Journal of Coal Geology, **217**: 103–319.

Knauth, L.P., 1998. Salinity history of the Earth's early ocean. Nature, **395**: 554–555.

Knauth, L.P., 2005. Temperature and salinity history of the Precambrian ocean: implications for the course of microbial evolution. Palaeogeography Palaeoclimatology Palaeoecology, **219**: 53–69.

Kovalevich, V.M., Peryt, T.M., Petrichenko, O.I., 1998. Secular variation in seawater chemistry during the Phanerozoic as indicated by brine inclusions in halite. The Journal of Geology, **106**: 695–712.

Kovalevych, V.M., Peryt, T.M., Carmona, V., Sydor, D.V., Vovnyuk S.V., Halas, S., 2002. Evolution of Permian seawater: evidence from fluid inclusions in halite. Neues Jahrbuch für Mineralogie Abhandlungen, **178**: 27–62.

Kovalevych, V.M., Marshall, T., Peryt, T.M., Petrychenko, O.Y., Zhukova, S., 2006. Chemical composition of seawater in Neoproterozoic: results of fluid inclusion study of halite from the Salt Range (Pakistan) and Amadeus Basin (Australia). Precambrian Research, **144**: 39–51.

Kovalevych, V.M., Paul, J., Peryt, T.M., 2009. Fluid inclusions in halite from the Röt (lower Triassic) salt deposit in central Germany: evidence for seawater chemistry and conditions of salt deposition and recrystallization. Carbonates and Evaporites, **24**: 45–57.

Li, Q.K., Fan, Q.S., Shan, F.S., Qin, Z.J., Li, J.S., Yuan, Q., Wei, H.C., Wang, M.X., Li, Y.Q., Shi, G.C., 2018. The variation of sulfur isotope in marine-continental evaporites and its geochemical applications (in Chinese with English summary). Journal of Salt Lake Research, **26**: 73–79.

Longinelli, A., 1989. Oxygen-18 and sulphur-34 in dissolved oceanic sulphate and phosphate. In: Handbook of environmental isotope geochemistry, **3** (eds. P. Fritz and J.C., Fontes)**:** 219–255. Elsevier, Amsterdam.

Losey, A., Benison, K.C., 2000. Silurian paleoclimate data through fluid inclusions in the Salina Formation halite of the Michigan Basin. Carbonates and Evaporites, **15**: 28–36.

Lowenstein, T.K., Timofeeff, M.N., Brennan, S.T., Hardie, L.A., Demicco, R.V., 2001. Oscillations in Phanerozoic seawater chemistry: evidence from fluid inclusions. Science, **294**: 1086–1088.

Mazumdar, A., Bhattacharya, S.K., 2004. Stable isotopic study of late Neoproterozoic-early Cambrian(?) sediments from Nagaur--Ganganagar basin, western India: possible signatures of global and regional C-isotopic events. Geochemical Journal, **38**: 163–175.

Mazumdar, A., Strauss, H., 2006. Sulfur and strontium isotopic compositions of carbonate and evaporite rocks from the late Neoproterozoic-early Cambrian Bilara Group (Nagaur Basin, India): constraints on intrabasinal correlation and global sulfur cycle. Precambrian Research, **149**: 217–230.

Mazumdar, A., Goldberg, T., Strauss, H., 2008. Abiotic oxidation of pyrite by Fe (III) in acidic media and its implications for sulfur isotope measurements of lattice-bound sulfate in sediments. Chemical Geology, **253**: 30–37.

Mello, M.R., Mohriak, W.U., Koutsoukos, E.A.M., Figueira, J.C.A., 1991. Brazilian and West African oils: generation, migration, accumulation and correlation. Proceedings of the Thirteenth World Petroleum Congress, New York, John Wiley: 153–164.

Meng, F.W., Zhang, Z.L., Schiffbauer, J.D., Zhuo, Q.G., Zhao, M.J., Ni, P., Liu, W.H., Ahsan, N., Rehman, S.U., 2019. The Yudomski event and subsequent decline: new evidence from $\delta^{34}S$ data of lower and middle Cambrian evaporites in the Tarim Basin, western China. Carbonates and Evaporites, **34**: 1117–1129.

Meng, F.W., Ni, P., Schiffbauer, J.D., Yuan, X.L., Zhou, C.M., Wang, Y.G., Xia, M.L., 2011a. Ediacaran seawater temperature: evidence from inclusions of Sinian halite. Precambrian Research, **184**: 63–69.

Meng, F.W., Ni, P., Wang, T.G., Yan, K., Wang, G.G., Zhao, C., Song, W.M., 2011b. Chemical composition of the ancient lake at Jintan Salt Mine: evidence from fluid inclusions in halite (in Chinese with English summary). Acta Micropalaeontologica Sinica, **28**: 324–328.

Meng, F.W., Liu, C.L., Ni, P., 2012. To forecast sylvite deposits using the chemistry of fluid inclusions in halite (in Chinese with English summary). Acta Micropalaeontologica Sinica, **29**: 62–69.

Meng, F.W., Galamay, A.R., Ni, P., Yang, C.H., Li, Y.P., Zhuo, Q.G., 2014. The major composition of a middle-late Eocene salt lake in the Yunying depression of Jianghan Basin of Middle China based on analyses of fluid inclusions in halite. Journal of Asian Earth Sciences, **85**: 97–105.

Meng, F., Zhang, Y., Galamay, A.R., Bukowski, K., Ni, P., Xing, E., Ji, L., 2018. Ordovician seawater composition: evidence from fluid inclusions in halite. Geological Quarterly, **62** (2): 344–352.

Misi, A., Veizer, J., 1998. Neoproterozoic carbonate sequences of the Una Group, Irece Basin, Brazil: chemostratigraphy, age and correlations. Precambrian Research, **89**: 87–100.

Och, L.M., Cremonese, L., Shields-Zhou, G.A., Poulton, S.W., Struck, U., Ling, H., Strauss, H., Zhu, M., 2016. Palaeoceanographic controls on spatial redox distribution over the Yangtze Platform during the Ediacaran-Cambrian transition. Sedimentology, **63**: 378–410.

Paytan, A., Gray, E.T., Ma, Z., Erhardt, A., Faul, K., 2012. Application of sulphur isotopes for stratigraphic correlation. Isotopes in Environmental and Health Studies, **48**: 195–206.

Peryt, T.M., Hałas, S., Kovalevych, V.M., Petrychenko, O.Y., Dzhinoridze, N.M., 2005. The sulphur and oxygen isotopic composition of Lower Cambrian anhydrites in East Siberia. Geological Quarterly, **49** (2): 235–242.

Peters, K.E., Clark, M.E., Das Gupta, U., Lee, C.Y., 1995. Recognition of an Infracambrian source rock based on biomarkers in the Baghewala-1 oil, India. AAPG Bulletin, **79**: 1481–1494.

Petrychenko, Y., Peryt, T.M., 2004. Geochemical conditions of deposition in the Upper Devonian Prypiac' and Dnipro-Donets evaporite basins (Belarus and Ukraine). Journal of Geology, **112**: 577–592.

Petrychenko, O.Y., Peryt, T.M., Chechel, W.I., 2005. Early Cambrian seawater chemistry from fluid inclusions in halite from Siberian evaporites. Chemical Geology, **219**: 149–161.

Present, T.M., Adkins, J.F., Fischer, W.W., 2020. Variability in sulfur isotope records of Phanerozoic seawater sulfate. Geophysical Research Letters, **47**. Art. No. e2020GL088766.

Raab, M., Spiro, B., 1991. Sulfur isotope variations during seawater evaporation with fractional crystallization. Chemical Geology, **86**: 323–333.

Sakai, H., 1972. Oxygen isotope ratios of some evaporites from Precambrian to Recent ages. Earth and Planetary Science Letters, **15**: 201–205.

Satterfield, C.L., Lowenstein, T.K., Vreeland, R.H., Rosenzweig, W.D., 2005. Paleobrine temperatures, chemistries, and paleoenvironments of Silurian Salina Formation F-1 Salt, Michigan Basin, USA, from petrography and fluid inclusions in halite. Journal of Sedimentary Research, **75**: 534-546.

Schröder, S., Schreiber, C., Amthor, J.E., Matter, A., 2004. Stratigraphy and environmental conditions of the terminal Neoproterozoic–Cambrian period in Oman: evidence from sulphur isotopes. Journal of the Geological Society, **161**: 489–499.

Schröder, S., Bekker, A., Beukes, N.J., Strauss, H., van Niekerk, H.S., 2008. Rise in seawater sulphate concentration associated with the Paleoproterozoic positive carbon isotope excursion: evidence from sulphate evaporites in the ~2.2–2.1 Gyr shallow-marine Lucknow Formation, South Africa. Terra Nova, **20**: 108–117.

Shah, S.M.I., 1977. Stratigraphy of Pakistan. Memoir of Geological Survey of Pakistan, **12**: 1–138.

Shah, S.M.I., 2009. Stratigraphy of Pakistan. Memoir of Geological Survey of Pakistan, **22**: 1–381.

Shields, G.A., Strauss, H., Howe, S.S., Siegmund, H., 1999. Sulphur isotope composition of sedimentary phosphorites from the basal Cambrian of China: implications for Neoproterozoic-Cambrian biogeochemical cycling. Journal of the Geological Society, **156**: 943–956.

Shields, G.A., Mills, B.J.W., 2019. Sulfur cycle imbalance and environmental change during the Ediacaran Period. Estudios Geológicos, **75**, https://doi.org/10.3989/egeol.43605.569

Shields, G., Kimura, H., Yang, J.D., Gammon, P., 2004. Sulphur isotopic evolution of Neoproterozoic-Cambrian seawater: new francolite-bound sulphate $\delta^{34}S$ data and a critical appraisal of the existing record. Chemical Geology, **204**: 163–182.

Spear, N., Holland, H.D., Garcia-Veígas, J., Lowenstein, T.K., Giegengack, R., Peters, H., 2014. Analyses of fluid inclusions in Neoproterozoic marine halite provide oldest measurement of seawater chemistry. Geology, **42**: 103–106.

Strauss, H., 1993. The sulfur isotopic record of Precambrian sulfates: new data and a critical evaluation of the existing record. Precambrian Research, **63**: 225–246.

Strauss, H., 2003. Sulphur isotopes and the early Archaean sulphur cycle. Precambrian Research, **126**: 349–361.

Strauss, H., Banerjee, D.M., 1998. The sulphur isotopic composition of Neoproterozoic to early Cambrian seawater – evidence from the cyclic Hanseran evaporites, NW India. Mineralogical Magazine, **62A**: 1467–1468.

Strauss, H., Banerjee, D.M., Kumar, V., 2001. The sulfur isotopic composition of Neoproterozoic to early Cambrian seawater—evidence from the cyclic Hanseran evaporites, NW India. Chemical Geology, **175**: 17–28.

Sweeney, R.E., Kaplan, I.R., 1980. Stable isotope composition of dissolved sulfate and hydrogen sulfide in the Black Sea. Marine Chemistry, **9**: 145–152.

Thode, H.G., Monster, J., Dunford, H., 1961. Sulphur isotope geochemistry. Geochimica et Cosmochimica Acta, **25**: 159–174.

Tostevin, R., He, T., Turchyn, A.V., Wood, R.A., Penny, A.M., Bowyer, F., Antler, G., Shields, G.A., 2017. Constraints on the late Ediacaran sulfur cycle from carbonate associated sulfate. Precambrian Research, **290**: 113–125.

Wang, G.L., Wang, T.G., Han, K.Y., Wang, L.S., Shi, S.B., 2015. Recognition of a novel Precambrian petroleum system based on isotopic and biomarker evidence in Yangtze platform, South China. Marine and Petroleum Geology, **68**: 414–426.

Warren, J.K., 2016. Evaporites: a Geological Compendium (2nd edition). Springer, Berlin.

Wynne, A.B., 1878. Geology of the Salt Range in the Punjab. Memoirs of the Geological Survey of India, **14**: 1–313.

Yao, W.Q., Wortmann, U.G., Paytan, A., 2019. Sulfur isotopes – use for stratigraphy during times of rapid perturbations. Stratigraphy and Timescales, **4**: 1**–**33.

Zhang, T.G., Chun, X.L., Zhang, Q.R., Feng, L.J., Huo, W.G., 2003. Variations of sulfur and carbon isotopes in seawater during the Doushantuo stage in late Neoproterozoic. Chinese Science Bulletin, **48**: 1375–1380.

Zhang, T.G., Chun, X.L., Zhang, Q.R., Feng, L.J., Huo, W.G., 2004. The sulphur and carbon isotope records in carbonates of the Dengying Formation in the Yangtze Platform, China. Acta Petrologica Sinica, **20**: 717–724.

Zhao, Z.Q., Xing, Y.S., Ma, G.G., Yu, W., Wang, Z., 1980. The Sinian System of Eastern Yangtze Gorges, Hubei (in Chinese with English summary). In: Research on Precambrian Geology: Sinian Suberathem in China (ed. Y.L. Wang): 31–55. Tianjin Science and Technology Press, Tianjin.